Journal of Autoimmunity 146 (2024) 103234

Contents lists available at ScienceDirect

Journal of Autoimmunity

journal homepage: www.elsevier.com/locate/jautimm

Single cell transcriptomics of cerebrospinal fluid cells from patients with recent-onset narcolepsy

Alina Huth [a,b], Ikram Ayoub [c], Lucie Barateau [d], Lisa Ann Gerdes [a,b,e], Dany Severac [f], Stefan Krebs [g], Helmut Blum [g], Hayrettin Tumani [h], Jürgen Haas [i], Brigitte Wildemann [i], Tania Kümpfel [a,b], Eduardo Beltrán [a,b,e], Roland S. Liblau [c], Yves Dauvilliers [d], Klaus Dornmair [a,b,e,*]

[a] Institute of Clinical Neuroimmunology, University Hospital, LMU Munich, Munich, Germany
[b] Biomedical Center (BMC), Faculty of Medicine, LMU Munich, Martinsried, Germany
[c] Toulouse Institute for Infectious and Inflammatory Diseases (Infinity), University of Toulouse, CNRS, INSERM, Toulouse, France
[d] Sleep-Wake Disorders Center, Department of Neurology, Gui-de-Chauliac Hospital, Institute for Neurosciences of Montpellier INM, INSERM, University of Montpellier, Montpellier, France
[e] Munich Cluster of Systems Neurology (SyNergy), Munich, Germany
[f] GenomiX, MGX, BioCampus Montpellier, CNRS, INSERM, Univ. Montpellier, F-34094, Montpellier, France
[g] Laboratory for Functional Genome Analysis (LAFUGA), Gene Center of the LMU, Munich, Germany
[h] Department of Neurology, University Hospital Ulm, Ulm, Germany
[i] Molecular Neuroimmunology Group, Department of Neurology, University of Heidelberg, Heidelberg, Germany

ARTICLE INFO

Keywords:
Narcolepsy
T cells
Cerebrospinal fluid (CSF)
Single-cell RNA sequencing (scRNAseq)
Transcriptomics

ABSTRACT

Narcolepsy is a rare cause of hypersomnolence and may be associated or not with cataplexy, i.e. sudden muscle weakness. These forms are designated narcolepsy-type 1 (NT1) and -type 2 (NT2), respectively. Notable characteristics of narcolepsy are that most patients carry the *HLA-DQB1*06:02* allele and NT1-patients have strongly decreased levels of hypocretin-1 (synonym orexin-A) in the cerebrospinal fluid (CSF). The pathogenesis of narcolepsy is still not completely understood but the strong HLA-bias and increased frequencies of $CD4^+$ T cells reactive to hypocretin in the peripheral blood suggest autoimmune processes in the hypothalamus. Here we analyzed the transcriptomes of CSF-cells from twelve NT1 and two NT2 patients by single cell RNAseq (scRNAseq). As controls, we used CSF cells from patients with multiple sclerosis, radiologically isolated syndrome, and idiopathic intracranial hypertension. From 27,255 CSF cells, we identified 20 clusters of different cell types and found significant differences in three $CD4^+$ T cell and one monocyte clusters between narcolepsy and multiple sclerosis patients. Over 1000 genes were differentially regulated between patients with NT1 and other diseases. Surprisingly, the most strongly upregulated genes in narcolepsy patients as compared to controls were coding for the genome-encoded MTRNR2L12 and MTRNR2L8 peptides, which are homologous to the mitochondria-encoded HUMANIN peptide that is known playing a role in other neurological diseases including Alzheimer's disease.

1. Introduction

Narcolepsy is a rare chronic, central nervous system disorder of hypersomnolence characterized by excessive daytime sleepiness, which can be associated with cataplexy, disrupted nighttime sleep, hypnagogic/hypnopompic hallucinations, and sleep paralysis [1–3]. There are two major types of narcolepsy: narcolepsy type 1 (NT1) and narcolepsy type 2 (NT2). In contrast to NT2-patients, almost all patients with NT1 have cataplexy, dramatically decreased levels of hypocretin1 (synonym orexin-A) in the cerebrospinal fluid (CSF), and carry the *HLA-DQB1*06:02* allele [2–4]. This strong HLA-bias and the increased incidence of NT1 after vaccination against the 2009 H1N1 influenza virus strain [5] suggest that immunological mechanisms play a highly relevant role in the pathophysiology of NT1. Further, NT1 is associated

* Corresponding author. Institute of Clinical Neuroimmunology, LMU Munich, Biomedical Center, Grosshadernerstr. 9, D-82152, Martinsried, Germany.
E-mail address: Klaus.Dornmair@med.uni-muenchen.de (K. Dornmair).

https://doi.org/10.1016/j.jaut.2024.103234
Received 21 October 2023; Received in revised form 23 March 2024; Accepted 16 April 2024
Available online 24 April 2024

with polymorphisms within the TCR alpha and beta loci [3,6], and preferred usage of particular TCR alpha-chains by $CD4^+$ T cell clones was observed in the blood [7]. However, overall, the TCR repertoire is quite broad and no particular bias in the repertoire of TCR beta-chains has been found in peripheral blood [7,8]. However, increased frequencies of blood $CD4^+$ T cells that recognize hypocretin and its post-translationally modified form were observed [8,9]. Given the very strong evidence for an immune-mediated process in NT1 and emerging data pointing to an autoimmune mechanism, assessing the level and nature of the inflammatory process in the target tissue (the hypothalamus, containing all hypocretin neurons) or in proximity to the target tissue becomes an important challenge.

To shed further light on the pathogenesis of narcolepsy we here analyzed the transcriptome of single cells isolated from CSF of patients with NT1 and NT2 with recent disease onset. As controls, we used CSF cells from patients with multiple sclerosis (MS), radiologically isolated syndrome (RIS), and idiopathic intracranial hypertension (IIH), i.e. from patients with a chronic inflammatory and a non-inflammatory neurological disease, respectively. We could distinguish 20 clusters of different cell types and identified significant differences between NT1 and MS in three clusters of $CD4^+$ T cells and one monocyte cluster. Analysis of differentially expressed genes (DEG) revealed more than 1000 genes that were differentially regulated between NT1, NT2, MS and IIH. Particularly strongly upregulated in NT1 as compared to MS and IIH were the genome-encoded MTRNR2L12 and *MTRNR2L8* genes [10], which are highly homologous to the well-investigated mitochondria-encoded *HUMANIN* gene [11].

2. Materials and methods

2.1. Patients

We collected CSF from patients with NT1, NT2, MS and IIH. Twelve patients (8 females, mean age at 19.1 y. o. ± 10.6, range 8–39) with NT1 presenting with excessive daytime sleepiness, typical cataplexy and hypocretin deficiency were included. All patients had CSF hypocretin-1 levels below 110 pg/ml (all except three were below detection level) and all but one were *HLA-DQ-B1*06:02* positive. The delay from excessive daytime sleepiness (first symptom) to CSF collection was remarkably short, with a mean of 12.25 months ±8.05 (range 5–36). Two patients (2 males, aged 14 and 24) with NT2 were included: one with atypical cataplexy, *HLA-DQB1*06:02* positive, and intermediate CSF hypocretin-1 level (144 pg/ml); and the other without cataplexy, *HLA-DQB1*06:02* negative and normal CSF-hypocretin-1 level (234 pg/ml). None of the narcoleptic patients received vaccination against the 2009H1N1 influenza virus strain.

In the MS-related group, we included five patients (4 females, mean age at 30.2 y. o. ± 6.02, range 24–40): three patients with established MS and two patients with radiologically isolated syndrome (RIS) to avoid a too strong inflammatory bias of the cohort. All patients with MS and RIS were positive for *HLA-DQB1*06:02*. Further, we included five patients (5 females, mean age at 35.8 y. o. ± 13.92, range 25–50) with IIH. All MS, RIS, and IIH patients were treatment naïve. Data of B cells and plasmablasts from patients RIS-2 and RIS-3 were published [12]. Data of $CD4^+$ T cells from patient MS-5 and all IIH patients were published [13].

The studies involving NAR patients were reviewed and approved by Comité de Protection des Personnes Nord-Ouest I, CPP 00035/200018 "Constitution of a cohort and of a clinical, neurophysiological and biological bank of rare hypersomnolence disorders" called SOMNOBANK (NCT03998020) that includes adults and children above 6 years and older. The study on MS and IIH patients was approved by the local ethics committee of the Ludwig-Maximilian University Munich (projects no. 163-16 and 18-419). Written informed consent was granted by all participants included in the study, and their parents for children with narcolepsy.

2.2. Isolation of cells, next generation sequencing

CSF cells from all patients were processed immediately after lumbar puncture except cells from RIS-2, MS-12, MS-13, NT2-1, NT1-3, NT1-13, NT1-14, which were frozen alive at −80 °C and stored in liquid nitrogen. The frozen samples contained 4963 cells (709 cells/patient) and the directly processed 22292 cells (1,311 cells/patient). It has been shown that although the total cell numbers are decreased upon freezing, the correlation of cluster distribution and gene expression from frozen vs. fresh CSF samples remains strongly correlated [14]. Comparisons of unique molecular identifiers, expressed genes, and mitochondrial gene expression per cell between frozen and fresh cells show no significant differences (Supplementary Fig. S1). Single cells from CSF were labelled with barcoded antibodies targeting CD4 or CD8α using the TotalSeq-C with 10× Feature Barcoding Technology (Biolegend) as described in 10× Genomics protocol CG000149 (Rev B).

Single-cell gene expression (GEX), αβ-T-cell receptor (TCR), and cell surface protein (CSP) libraries were prepared using the 10× Genomics platform according to protocol CG000208 (Rev F). All antibody-labelled CSF cells from each sample were used as input. Nuclease-free water was added to the barcode antibody-labelled cells to a final volume of 37.8 μL and the protocol was carried out with the minor alterations described [15]. The sequencing depth was 19,542–823,974 (mean: 176,279) reads per cell for the GEX libraries, 3,656–745,017 (mean: 95,677) reads per cell for the TCR libraries, and 647 - 341,911 (mean: 63,609) reads per cell for the CSP libraries.

2.3. Pre-processing of single-cell sequencing data

Raw data obtained from sequencing was pre-processed and aligned to the human reference genome GRCh38-2020-A (GEX) or GRCh38-alts-ensembl-5.0.0 (TCR) using Cell Ranger (10× Genomics, version 6.0.2) [16] as described [17]. The optimum numbers of PCs to use for each clustering step were derived from an Elbow plot for each dataset (i.e., all CSF cells, $CD4^+$ T cells only, and $CD8^+$ T cells only). The optimal resolution was determined as the minimum resolution between 0.4 and 1.0 that yielded clusters that contained unique and distinguishable immune cell types based on cluster marker gene expression. Pre-processed data were then further processed and analyzed in JupyterLab (version 3.2.1 URL https://www.R-project.org/) using an R kernel (R version 4.1.3, http://www.rstudio.com/) and the R package Seurat (version 4.1.1). In summary, data from GEX and CSP libraries were combined for each sample, quality-filtered to remove low-quality cells, doublets, and dead cells according to the recommendations of the Seurat Guided Clustering Tutorial (Standard pre-processing workflow). Thus, cells were kept only if the contained >500 and < 20,000 RNA molecules, >200 and <2,500 genes, and ≤7.5 % mitochondrial RNA. Read counts from GEX and CSP assays were normalized by sample using the NormalizeData-function with normalization-method set to "LogNormalize" and "CLR", respectively. The T-cell clusters within the CSF immune cells were identified by expression of CD3D and CD3E. Cells that were not located in the T-cell clusters or did not express at least one TCR alpha- or beta-chain were excluded. $CD8^+$ and $CD4^+$ T-cell subsets were identified based on normalized CSP barcode read count data. Cells that were at least 1.5-fold enriched in CD8A compared to CD4 were assigned the cell type $CD8^+$ T cells. Conversely, cells that were at least 1.5-fold depleted in CD8A compared to CD4 were assigned the cell type $CD4^+$ T cells. The remaining cells were assigned to $CD8^+$ T cells if their normalized CD8A RNA count in the RNA assay was ≥0.8 and CD4 expression was <0.2, and to $CD4^+$ T cells if the opposite was the case. Cells that could not be assigned to $CD4^+$ T cells or $CD8^+$ T cells were categorized as ambiguous. T cells that express at least one identical TCR alpha- or beta-chain were defined as clonotypes [15]. T cell clones were considered expanded if their TCR clonotype was found at least twice by Cell Ranger (i.e. clonotype frequency >1) as described [15].

2.4. Clustering and identification of immune cell types and differential gene expression

Variable features were identified, and data was scaled using the Seurat pipeline. Principal component analysis (PCA) was performed and data from the individual samples was integrated using the R package harmony (version 0.1.0) [18]. After integration, UMAP was used for dimensional reduction. Clustering was performed using Seurat's shared nearest neighbour algorithm with 25 PCs and a resolution of 0.9. Immune cell subsets were identified based on differentially expressed genes by each cluster as identified by Seurat's FindAllMarkers function, based on expression of established immune marker genes, and based on assignment to the $CD4^+$ and $CD8^+$ T-cell subset. For separated clustering of $CD8^+$ and $CD4^+$ T cells, clusters of single cells that were assigned to these cell types were extracted from the CSF data ($CD8^+$ T cells: CSF clusters 3, 7, 17; $CD4^+$ T cells: clusters 0, 1, 2, 6, 9, 13). Subsequently, the cell subsets were re-clustered and more precise immune cell types were identified as described above starting from variable feature selection. $CD8^+$ T cells were clustered based on 25 PCs at a resolution of 0.5. The $CD8^+$ MAIT T-cell cluster was identified based on high prevalence of cells expressing TRA chains TRAV1-2 and TRAJ12, TRAJ20, TRAJ22 together with TRBV6 or TRBV20-1 genes [19]. $CD4^+$ T cells were clustered based on 35 PCs at a resolution of 0.5. DEGs between NT1 and control study groups were identified using Seurat's FindMarkers-function. Prior to DEG identification, cells were downsampled to 300 cells (CSF) and 100 cells ($CD4^+$ T cells) per sample to give similar weight to all samples. The relatively low input cell numbers and downsampling of cells to 300 or 100 cells per sample for DEG-analysis make doublets further highly unlikely.

2.5. Pathway analysis

Pathway Analysis was performed on the differentially expressed genes (p.adjusted$<$0.05) and using the R package ClusterProfiler [20].

2.6. Data visualization

UMAP plots, Heatmaps showing gene expression per cluster or cell type, and violin plots were created using Seurat. Dot plots, volcano plots, and remaining heatmaps were created in RStudio (version 2022.02.1) using the R packages ggplot2 (version 3.3.6), cowplot (version 1.1.1), and ComplexHeatmap (version 2.10.0).

2.7. Statistics

P values for different cell type and cluster compositions between cohorts were calculated using two-sample t-tests and adjusted with the Holm–Bonferroni method. P values for differential gene expression were calculated using Wilcoxon Rank Sum test and adjusted via Bonferroni correction across all genes in the dataset.

3. Results

3.1. Cellular diversity in the CSF of patients with narcolepsy, MS, and IIH

We analyzed CSF samples from 12 patients with recent-onset NT1, two patients with recent-onset NT2, and 5 patients with IIH. Additionally, two patients with RIS and three patients with established MS, all treatment-naïve, were combined as one MS group. Clinical data and numbers of cells analyzed after quality control and filtering per patient are shown (Table 1 and Supplementary Table S1A). A Uniform Manifold Approximation and Projection (UMAP) plot comprising all 27,255 cells for which reliable scRNAseq data were obtained is displayed in Fig. 1A. We identified 20 clusters of different cell numbers (Supplementary Table S1B), which can be assigned to 10 defined immune cell types (Supplementary Table S1C). To assign cell types to each cluster, we plotted the most strongly expressed genes of each cluster in a heatmap (Fig. 1B) and deduced the relevant cell types (Fig. 1C). The marker genes for CSF cell types and T are listed in Supplementary Table S2. This revealed six clusters of $CD4^+$ T cells (clusters number #0, 1, 2, 6, 9, 13) and three clusters of $CD8^+$ T cells (#3, 7, 17). Clusters 1 and 2 were very similar to cluster 0 showing a slightly higher expression of activation markers like granzymes (GZM) A and K, cluster 6 contained highly activated T cells expressing high levels of GZMK, GZMA, CXCR6, and cluster 9 comprised regulatory T cells, which notably express FOXP3 and TIGIT. $CD8^+$ T cells of cluster 3 showed higher levels of activation markers than those of cluster 17 and 7, while cluster 7 expressed higher levels of the tissue-resident memory T cell-associated transcription factor ZNF683/HOBIT. Further, the heatmap allowed us to identify 5 clusters of monocytes (#4, 5, 10, 14, 19), 2 of dendritic cells (#15, 18), and 1 cluster each of B cells (#11), plasmablasts (#16), NK cells (#8), and γδ T cells (#12).

To gain further insight into the cellular distributions, we plotted the cell counts of each cluster as percentages of the total cell counts (Fig. 2A) and cell types (Fig. 2B) of each patient in the NT1, NT2, MS, and IIH groups. As expected, in all patient groups, $CD4^+$ T cells were the most populated clusters followed by clusters with $CD8^+$ T cells. It is evident that the cell frequencies of the three highly populated clusters, encompassing naïve or slightly activated $CD4^+$ T cells (#0, 1, 2), were relatively higher in MS patients as compared to NT1 and IIH patients. The differences between MS and NT1 patients in clusters 0 and 1 were statistically significant, as well as the differences in cluster 9, i.e. in regulatory $CD4^+$ T cells, and in the monocyte cluster 5. The differences in cell frequencies in all other clusters were not significant between the three patient groups, including the remaining clusters with $CD4^+$ and $CD8^+$ T cells (#2, 6, 13 and #3, 7, 17, respectively) and B cells and plasmablasts (#11, 16). Relative cell frequencies in patients with recent onset NT2, may be considered anecdotal, as only two patients were present in this group. Clusters containing activated $CD4^+$ and $CD8^+$ T cells (#3, 6, 17) as indicated by relatively high GZMA, GZMK and CXCR6 expression (Fig. 1B) showed comparable cell count percentages in all disease

Table 1
Clinical characteristics of the NT1, NT2, RIS, MS, and IIH patients. We list the designations of the patients (column 1), their sex (column 2), their age at the time of lumbar puncture (column 3), the time that passed since the first symptoms were observed (column 4), their *HLA-DQB1*06:02* status (column 5), and the hypocretin CSF levels for patients with NT1 or NT2 (column 6).

Participants	Sex	Age: Time of CSF (years)	Time since first symptoms (months)	HLA-DQB1*06:02	CSF hypocretin levels (pg/mL)
NT1-2	M	11	6	positive	14
NT1-3	M	33	13	positive	83
NT1-4	F	17	7	positive	<10
NT1-5	F	39	5	negative	<10
NT1-6	F	11	12	positive	13
NT1-8	M	29	36	positive	14
NT1-9	F	14	12	positive	<10
NT1-10	F	8	12	positive	<10
NT1-11	F	15	12	positive	17
NT1-12	F	32	12	positive	31
NT1-13	F	10	13	positive	54
NT1-14	M	10	7	positive	<10
NT2-1	M	24	72	positive	144
NT2-7	M	14	8	negative	234
RIS-2	M	24	6	positive	NA
RIS-3	F	28	5	positive	NA
MS-5	F	28	133	positive	NA
MS-12	F	40	233	positive	NA
MS-13	F	31	1	positive	NA
IIH-1	F	27	33	positive	NA
IIH-2	F	52	10	negative	NA
IIH-3	F	25	7	negative	NA
IIH-4	F	25	43	negative	NA
IIH-5	F	50	70	negative	NA

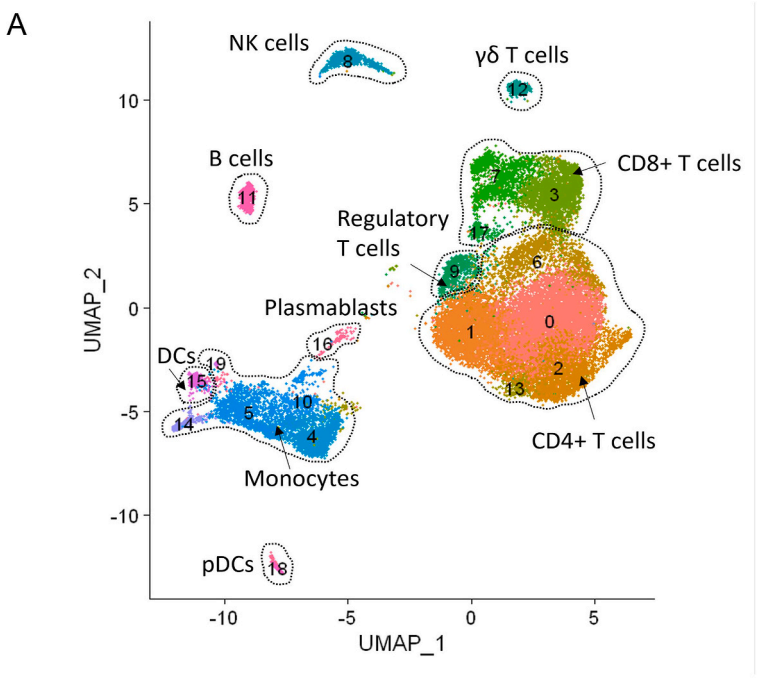

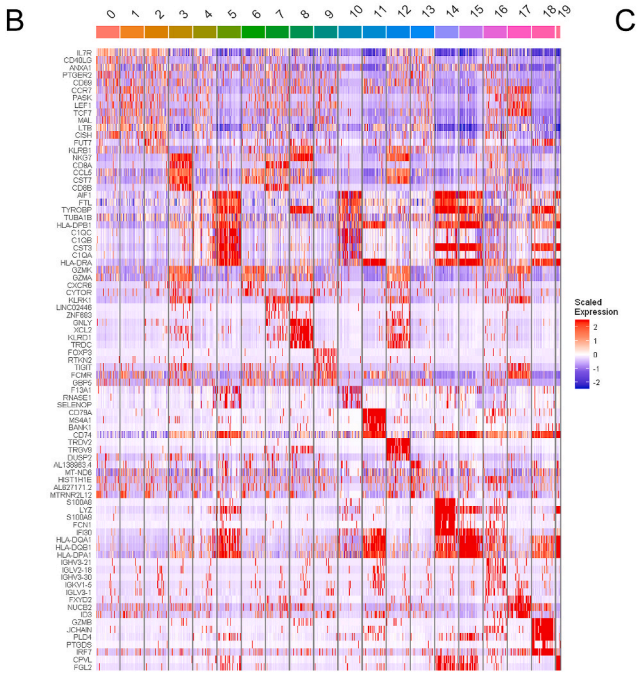

C

Cluster	Cell type
0	CD4+ T cells
1	CD4+ T cells
2	CD4+ T cells
3	CD8+ T cells
4	Monocytes
5	Monocytes
6	CD4+ T cells
7	CD8+ T cells
8	NK cells
9	Regulatory T cells
10	Monocytes
11	B cells
12	γδ T cells
13	CD4+ T cells
14	Monocytes
15	DCs
16	Plasmablasts
17	CD8+ T cells
18	pDCs
19	Monocytes

Fig. 1. Cellular composition of all CSF cells. Single cells were analyzed by scRNAseq and data were subjected to quality control and filtering. **A:** UMAP revealing 20 different clusters of CSF cells within the 27,255 single CSF cells from NT1 (n = 12), NT2 (n = 2), RIS (n = 2), MS (n = 3), and IIH (n = 5) patients (Supplementary Tables 1 and 2). Five different clusters of $CD4^+$ T cell, three clusters of $CD8^+$ T cell, four clusters of monocytes, two clusters of dendritic cells, and one cluster each of Tregs, γδ T cells, B cells, and plasmablasts are indicated. **B:** Heatmap displaying scaled expression of the five most distinctive marker genes for each of the 20 clusters. For each cluster, 100 randomly chosen cells are displayed. Cluster 19 consisted of only 18 cells, causing a narrower column. The colors and numbers on top refer to the cluster numbers from Fig. 1A. Gene names are shown on the left. **C:** Assignment of clusters to immune cell types based on the distinctive marker genes shown in Fig. 1B.

groups. Overall, we uncovered significant differences only between NT1 and MS patients, whereas the CSF cell composition in NT1 samples is quite similar to that of IIH.

3.2. *Gene expression profiles of $CD4^+$ and $CD8^+$ T cell subsets*

Next, we analyzed gene expression patterns from $CD4^+$ and $CD8^+$ T cells individually. CSF cells were assigned to the $CD4^+$ and $CD8^+$ T cell subset based on the results obtained from anti-CD4 and anti-CD8A antibody labelling and expression levels of CD4 and CD8A genes. Cells that were not located in the T-cell clusters 0, 1, 2, 3, 6, 7, 9, 13, and 17 (Fig. 1A) or did not express at least one alpha- or beta-TCR chain were excluded. A UMAP of the 14,549 re-clustered CD4 T cells is shown in Fig. 3A. Due to re-clustering, the shapes of the clusters differ slightly

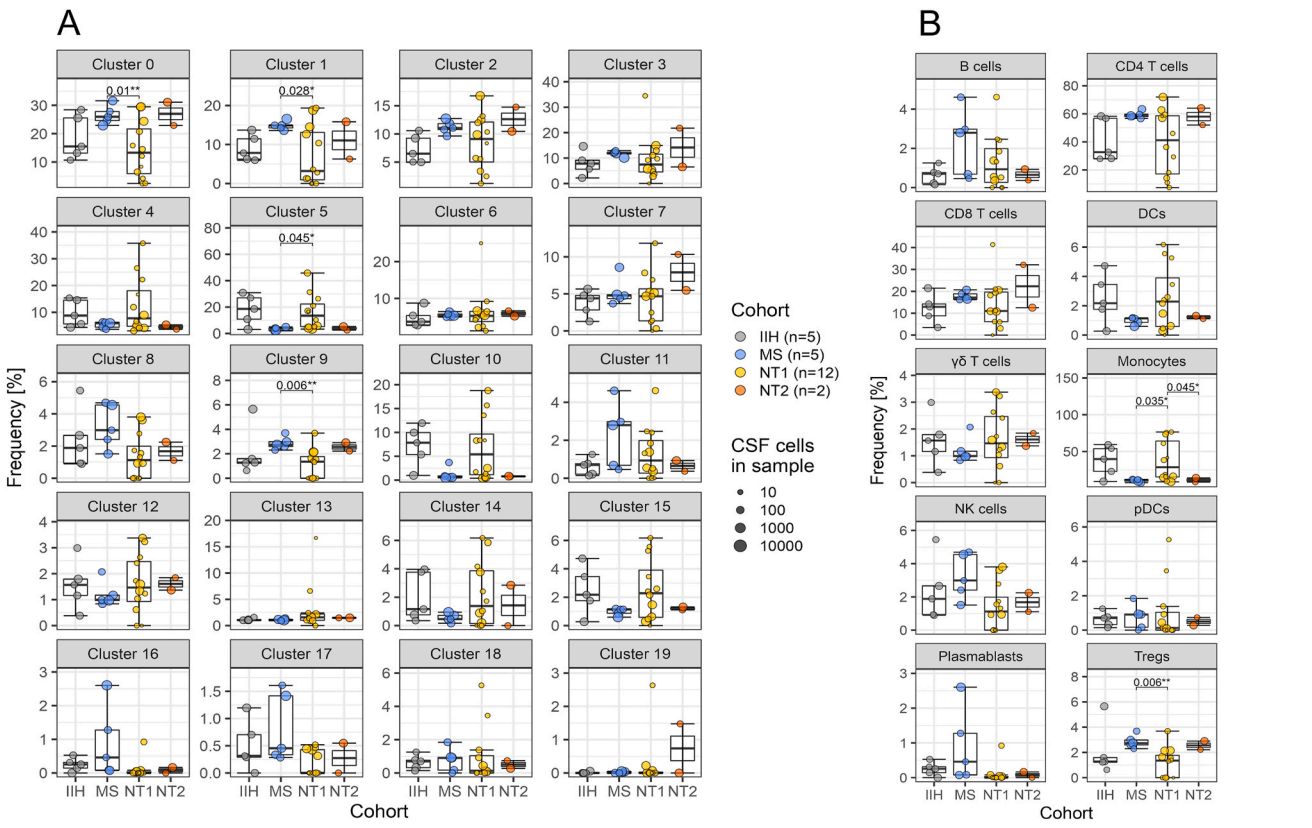

Fig. 2. Boxplots showing the cell counts of CSF clusters and cell types. A: Cell frequencies for clusters 0 to 19 are shown as percentages of the total CSF cell counts of NT1, NT2, MS, and IIH patients. B: Cell frequencies are shown for ten cell types (see Fig. 1 for assignment): B cells (cluster 11), $CD4^+$ T cells (clusters 0, 1, 2, 6, 13), $CD4^+$ Treg cells (cluster 9), $CD8^+$ T cells (clusters 3, 7, 17), dendritic cells (clusters 15, 18), γδ T cells (cluster 12), monocytes (clusters 4, 5, 10, 14, 19), NK cells (cluster 8), pDCs (cluster 18), and plasmablasts (cluster 16). Error bars (interquartile range), box plots, and median are indicated. The size of each dot reflects the total number of CSF cells in the corresponding sample. Holm-Bonferroni—adjusted p values are shown with their level of significance (* < 0.05; ** < 0.01; *** < 0.001) if the adjusted p value was <0.05 between any 2 groups. Note the different scales of the relative cell frequencies shown in percent of the total cell counts in each patient on the y-axis.

from the clusters in Fig. 1A. We could distinguish naïve T cells (Tnaive), Th1 central memory (Th1 Tcm), Th1 effector memory (Th1 Tem), Th17 (Th17), and regulatory T cells (Treg). This assignment of clusters to particular T cell types was based on preferential expression of marker genes as shown in Fig. 3B. We additionally compared the cell counts of each cluster as percentages of the total T cell counts of each patient in the NT1, NT2, MS, and IIH groups (Fig. 3C). None of the $CD4^+$ T cell subsets differed significantly between diseases. However, consistent with our analysis of all CSF cells above, there was a trend towards more Th1 Tem cells and less Tregs in NT1 samples compared to MS and IIH samples. A comparable analysis of 3,780 $CD8^+$ T cells (Fig. 4A–C) also revealed no significant differences in the $CD8^+$ T cell subsets between diseases. Usage of the hypervariable TCR chains allowed us to identify expanded $CD4^+$ T cell clones with identical TCR chains and to compare them to non-expanded clones. Expanded clonotypes of all patients are listed in Supplementary Table S3. Since clonal expansions likely arose from previous antigen contact, we analyzed expression patterns of activation-, apoptosis-, and exhaustion-markers genes from expanded $CD4^+$ T cell clones of Th1-Tcm and Th1-Tem, and Th17 subsets. However, we could not detect specific differences between IIH, MS, NT1 and NT2 patients (Supplementary Figs. S2A–C), which may be due to the low cell numbers available from CSF.

3.3. *Differentially expressed genes in CSF from NT1 versus MS and IIH patients*

We used volcano plots to visualize DEG of NT1 versus IIH (Fig. 5A), MS (Fig. 5B), and NT2 (Fig. 5C). Up- and downregulated genes in NT1 as compared to IIH, MS, and NT2 are shown in red color on the right side and in blue color on the left side of the plots, respectively. Analyzing all CSF cells, we identified 541 significant DEG in NT1 compared to IIH, 1,113 DEG in NT1 compared to MS, and 302 DEG in NT1 compared to NT2 (Supplementary Table S4, sheets 1 to 3). When focusing on genes that were not only significantly differentially expressed, but also possess an at least 2-fold higher or lower average gene expression in NT1 compared to one of the control cohorts, we found 12 genes to be strongly differentially regulated in NT1 compared to IIH, 61 genes compared to MS, and 33 genes compared to NT2 (highlighted in Supplementary Table S4, sheets 1 to 3). Many of the upregulated genes in MS as compared to NT1 were immunoglobulin genes, which is probably due to an increased humoral response in MS. The most significantly and most strongly upregulated gene in NT1 and NT2 compared to MS and to IIH were the two nucleus-encoded members of the HUMANIN (gene name MTRNR2) family, named MTRNR2L12 and MTRNR2L8 ("L" stands for "like") [10] (Fig. 5A and B and Supplementary Table S4, sheets 1 and 2). The mitochondria-encoded HUMANIN was not included in the standard reference genome GRCh38-2020-A, which is recommended by 10× Genomics for single cell analysis of human cells. Due to the high homologies within this gene-family, it may be possible that HUMANIN alone or in addition to MTRNR2L12 and -L8 is among the most highly DEGs in narcolepsy because the program Cell Ranger might have aligned the transcripts to next best fitting genes in the reference genome.

We next analyzed DEG between patient-groups among cells of the same CSF cell type (Fig. 5D–J). Dot plots of DEG are shown in specific cell types, namely for $CD4^+$ T cells (#0, 1, 2, 6, 13, Fig. 5D), $CD4^+$ Treg cells (#9, Fig. 5E), B cells and plasmablasts (#11, 16, Fig. 5F), $CD8^+$ T

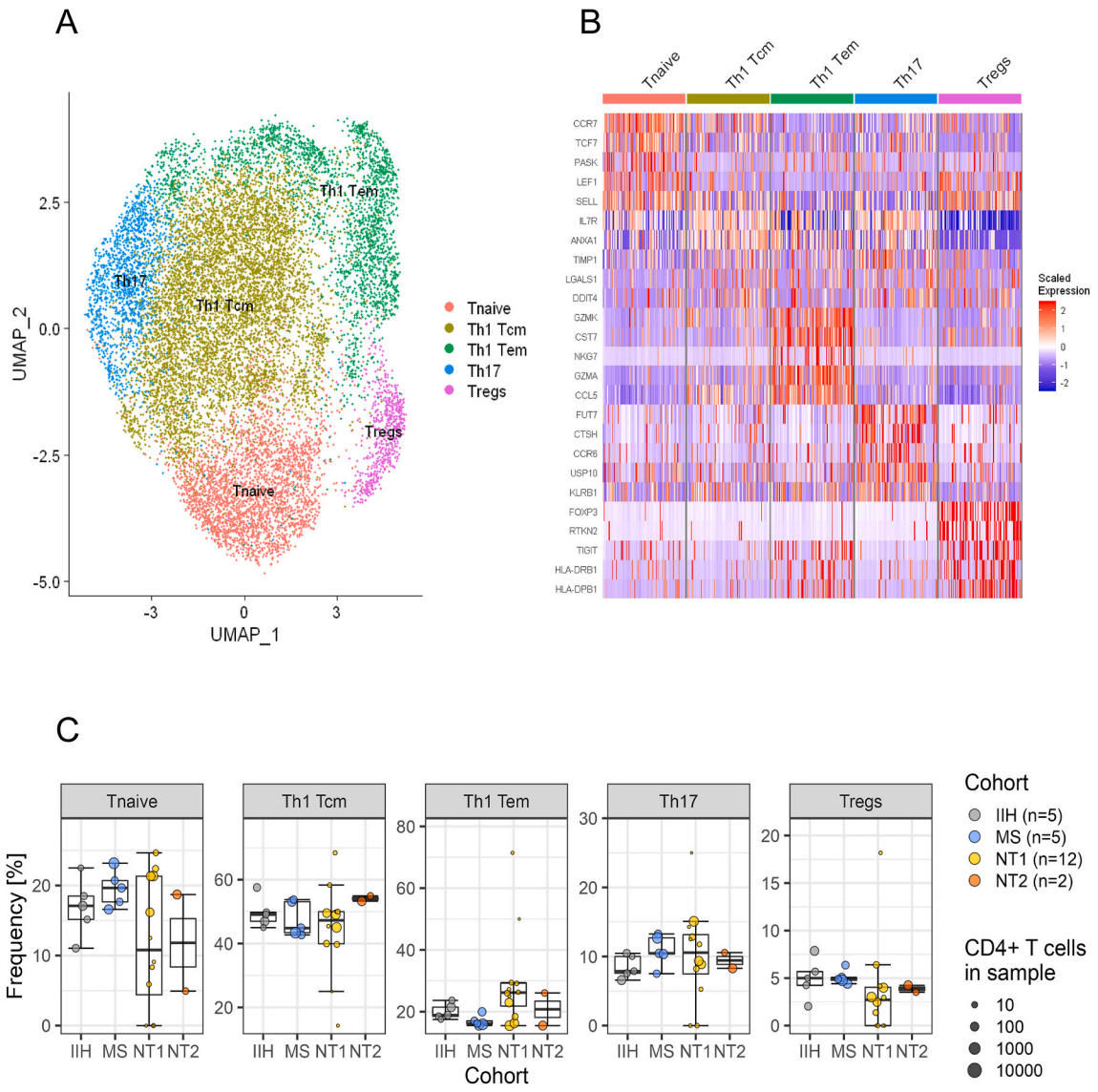

Fig. 3. Cellular composition of CD4$^+$ T cells. Integration of the scRNAseq sub-datasets and clustering was performed as described for CSF cells in Fig. 1. Cell types were identified by marker gene expression in the obtained clusters. **A:** UMAP showing five clusters identified from the 14,549 CD4$^+$ T cells of this dataset. Naïve T cells (Tnaive), Th1 central memory (Th1 Tcm), Th1 effector memory (Th1 Tem), Th17 (Th17), and regulatory T cells (Th1 Treg) are indicated. **B:** Heatmap displaying the scaled expression of the five most distinctive marker genes for each of the five CD4$^+$ cell types. The colors and designations on top refer to Fig. 2A. Gene names are shown on the left. **C:** CD4$^+$ T cell frequency by cell type. Boxplots showing the frequencies of cells from each of the five clusters shown in Fig. 2A as percentages of the total CSF CD4$^+$ T cell counts of NT1, NT2, MS, and IIH patients. Error bars (interquartile range), box plots, and median are indicated. The size of each dot reflects the total number of CD4$^+$ cells in the corresponding sample.

cells (#3, 7, 17, Fig. 5G), dendritic cells (#15, 18, Fig. 5H), γδ T cells (#12, Fig. 5I), and NK cells (#8, Fig. 5J). Dot plots of DEG of monocytes (#4, 5, 10, 14, 19), where particularly many DEG were detected, are shown in Supplementary Fig. S3. A comprehensive heatmap of DEG that differ between NT1 and the MS, IIH, and NT2 groups in different immune cell types is shown in Supplementary Fig. S4.

DEG of the 14,549 CD4$^+$ T cells (see Fig. 3) are depicted as volcano plots of NT1 versus IIH (Fig. 6A), MS (Fig. 6B), and NT2 (Fig. 6C). The DEG-pattern is similar to Fig. 5 with MTRNR2L12 and MTRNR2L8 being highly upregulated in NT1 as compared to IIH and MS. In Fig. 6D–H, we show dot plots of the most relevant DEG in each of the five CD4$^+$ T cell subsets identified in Fig. 3A. Supplementary Fig. S5 displays a heatmap of DEG in the different clusters and disease groups. Many genes were differentially upregulated in NT1 as compared to MS and IIH such as the ribosomal proteins RPS2 and NOP53, the mRNA-regulating gene ZFP36L2, and transcriptional regulators BTG1 and KLF2. CD69 and FOS, both being involved in T cell activation, were upregulated in MS as compared to NT1 and IIH, in agreement with the population of clusters with proinflammatory genes being higher in MS than in NT1 and IIH.

3.4. *High expression of MTRNR2L12 in narcolepsy*

Both, volcano- and dot plots for all cells and CD4$^+$ T cells (Figs. 5 and 6), as well as heat maps (Supplementary Figs. S3 and S4), underscore the prominence of MTRNR2L12 and MTRNR2L8, which were strongly overexpressed in NT1 and NT2 patients as compared to MS and IIH patients. Strikingly, both genes were overexpressed in all cell types (Fig. 5A and B and Fig. Supplementary S3), CD4$^+$ T cell (Fig. 6A and B and Supplementary Fig. S4), and CD8$^+$ T cell clusters (Fig. 5G). The other members of the MTRNR2L-group were expressed at very modest levels (Supplementary Fig. S6).

This was particularly evident when the expression of MTRNR2L12, the most highly upregulated gene, was analyzed in UMAP plots of the four disease groups (Fig. 7A–D). Its homolog MTRNR2L8 was also

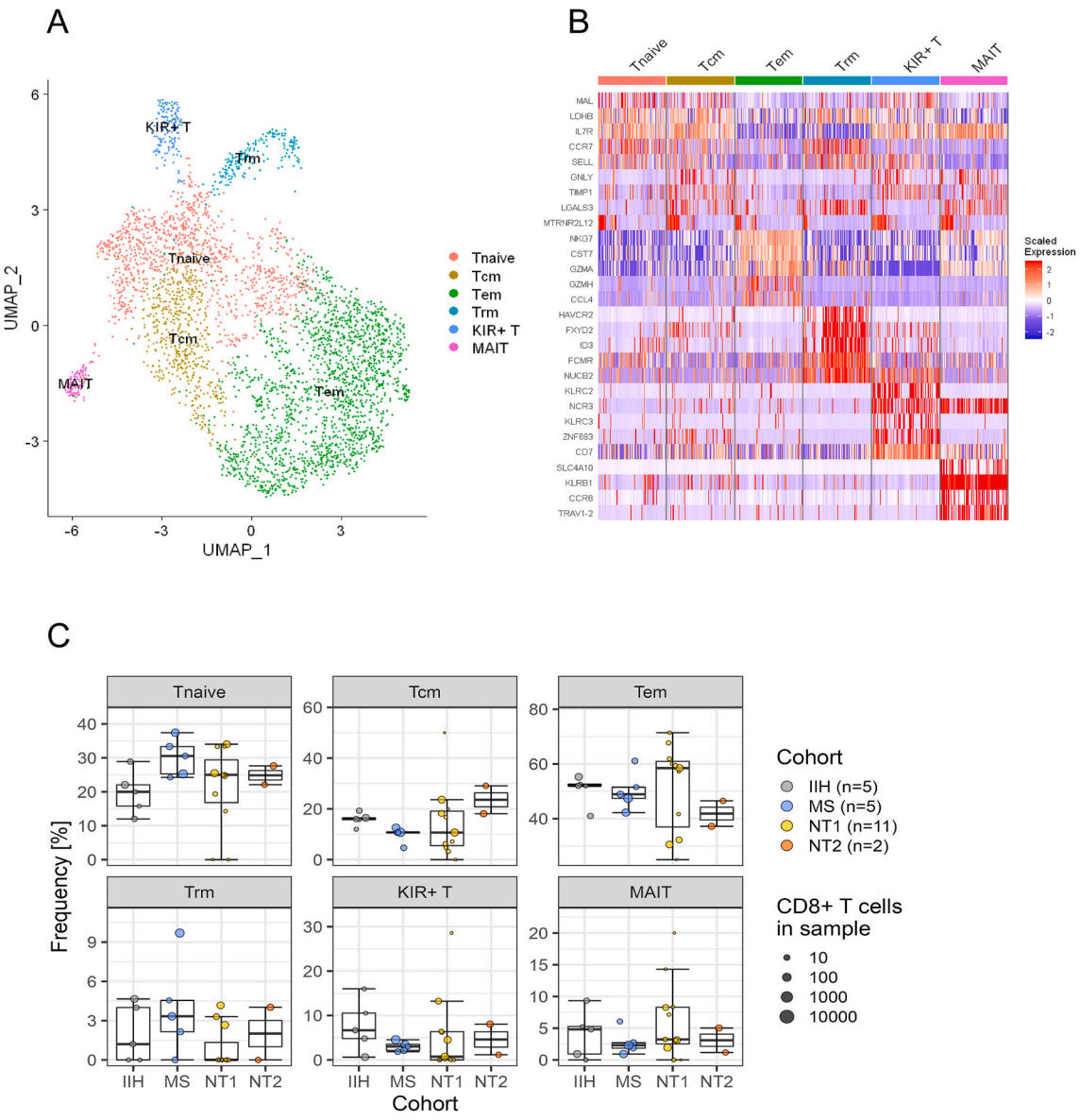

Fig. 4. Cellular composition of CD8$^+$ T cells. Integration of the scRNAseq sub-datasets and clustering was performed as described for CSF cells in Fig. 1. Cell types were identified by marker gene expression in the obtained clusters. **A:** UMAP showing the six CD8$^+$ T-cell types within the 3,780 CD8$^+$ T cells of this dataset. Effector memory T cells (Tem), naïve T cells (Tnaive), central memory T cells (Tcm), tissue-resident memory T cells (Trm), killer cell immunoglobulin-like receptors T cells (KIR$^+$ T), and mucosal associated invariant T cells (MAIT) are indicated. **B:** Heatmap displaying the scaled expression of the five most distinctive marker genes for each of the six CD8$^+$ T cell types. The colors and designations on top refer to Fig. 3A. Gene names are shown on the left. **C:** Boxplots showing the frequencies of cells in each of the six CD8$^+$ T cell types shown in Fig. 3A as percentages of the total CSF CD8$^+$ T cell counts of NT1, NT2, MS, and IIH patients. Error bars (interquartile range), box plots, and median are indicated. The size of each dot reflects the total number of CD8$^+$ T cells in the corresponding sample.

specifically expressed in CSF cells from NT1 and NT2 patients (Fig. 7E–H). Violin plots of all individual patients of each group reveal that MTRNR2L12 is highly expressed in 7 out of 12 NT1 and in 2 out of 2 NT2 patients (Fig. 7I). MTRNR2L8 is highly expressed in 5 out of 12 NT1 and in 1 out of 2 NT2 patients (Fig. 7J). Of note, both genes were not significantly expressed in any of the 5 MS and 5 IIH patients.

To gain insight into the biological perturbed pathways in NT1 patients, we performed pathway analysis using the R package ClusterProfiler focusing on the CD4$^+$ T cell clusters given their strongly suspected involvement in the NT1 pathogenesis [3]. We compared NT1 patients to the non-inflammatory control group (IIH). Results showed enrichment of pathways related to cytoplasmic translation and cytokine production (Supplementary Figs. S7A and B). Of particular interest, three pathways containing both the MTRNR2L8 and MTRNR2L12 genes were significantly enriched (Supplementary Fig. S7C). Among them, the "Negative regulation of signaling receptor activity" that contained the TNF gene in addition to MTRNR2L8, MTRNR2L12 and MTRNR2L1 was significantly enriched (Supplementary Fig. S7D).

4. Discussion

Here we compared the cellular landscapes of CSF cells from NT1, NT2, MS, and IIH patients in order to identify differences in gene-expression levels between narcoleptic and control patients, which might elucidate the pathogenesis of narcolepsy. Our study revealed that the CSF cell composition and gene expression levels in narcoleptic patients are more similar to the non-inflammatory disease IIH, while there were differences to the inflammatory disease MS. Notably, in this study, the MS patients were selected to share the NT1-associated *HLA-DQB1*06:02* allele, therefore significant differences between NT1 and

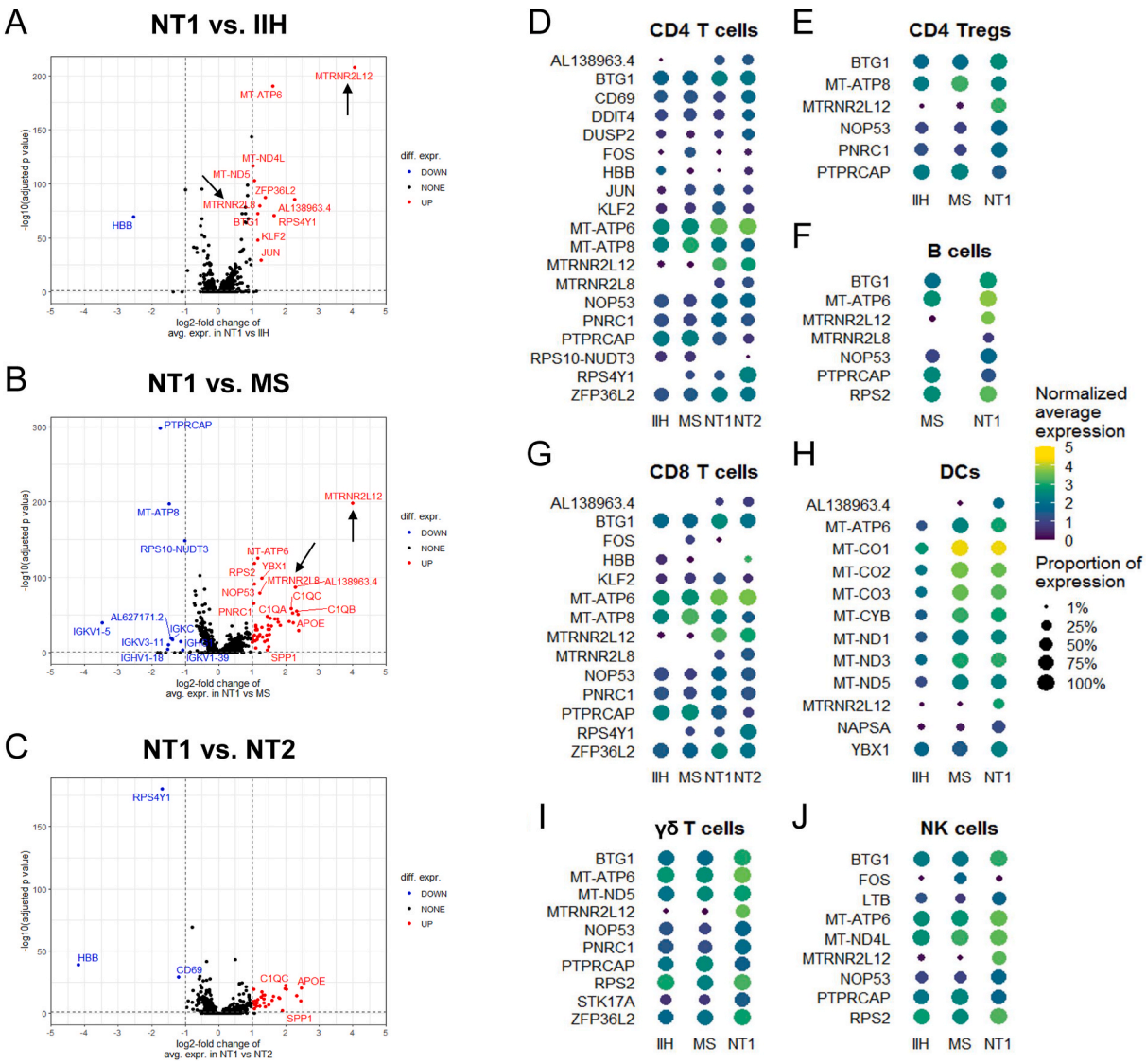

Fig. 5. Analysis of differentially expressed genes (DEG) in all CSF cells. Global DEG from gene expression comparisons: **A:** NT1 versus IIH, **B:** NT1 versus MS, and **C:** NT1 versus NT2 as volcano plots. CSF cells were downsampled to 300 cells per sample to give equal weight to each sample. Samples that contained less than 300 cells remained unchanged. Genes that were upregulated in NT1 as compared to IIH, MS, and NT2 are printed in red, while downregulated genes are shown in blue. MTRNR2L12 and MTRNR2L8 are indicated by black arrows. **D - J:** Subset-specific DEG were identified as differentially expressed in NT1 compared to any control cohort in a given CSF cell subset. Dot plots show DEG expression for each subset and cohort: **D:** $CD4^+$ T cells (clusters 0, 1, 2, 6, 13), **E:** $CD4^+$ Treg cells (cluster 9), **F:** B cells (cluster 11), **G:** $CD8^+$ T cells (clusters 3, 7, 17), **H:** dendritic cells (clusters 15), **I:** γδ T cells (clusters 12), and **J:** NK cells (cluster 8). Cell types for which insufficient cell numbers (plasmablasts, pDCs) were recovered in a patient group are not shown in these plots. The sizes of the dots are comparable for all cell types and represent the percentage of cells in the cell type expressing each gene. The color of each dot indicates the average expression level in cells of the cell type. Hemoglobin (HBB) transcripts derive from minor contamination with erythrocyte-RNA which is commonly seen in lumbar puncture samples [14] and unavoidable in clinical practice.

MS in gene expression levels and DEG are therefore not due to this HLA-allele. Consistent with the gene expression levels, we found upregulation of proinflammatory DEG in MS as compared to NT1 and IIH. This is probably due to the chronic marked inflammation ongoing in MS.

Single cell analyses in peripheral blood of NT1 patients using flow cytometry [21] or mass cytometry [22,23] revealed systemic activation of T cells, with, in particular, increased production of IL-2, IL-4, IL-13 and TNF by both antigen-experienced CD4 and CD8 T cells from NT1 patients as compared to controls following PMA/ionomycin stimulation. However, unbiased [24] and targeted [25] proteomics studies of the CSF of NT1 did not reveal significant difference in cytokine levels. Further single-cell transcriptomic analyses are warranted to determine whether the cytokine signaling pathways are dysregulated in NT1 patients.

The most striking DEG identified here were the HUMANIN-family members MTRNR2L12 and MTRNR2L8, which were both overexpressed in NT1 and NT2 as compared to MS and IIH. Both are 24 amino acid-long peptides encoded on chromosomes 3q11.2 and 11p15.3, respectively [10]. They belong to a group of 13 nucleus-encoded peptides [10]. As detailed above, HUMANIN was not included in the reference genome. Therefore, it is possible that HUMANIN is also one of the highest DEGs in narcolepsy but could not be detected here. The amino acid sequences of MTRNR2L12 and MTRNR2L8 are identical but their nucleotide sequences are different due to a silent exchange of adenine to guanine in position 54 [10]. The nucleotide sequences of HUMANIN differs at position 35, which leads to a substitution of serine by leucine in position 12. In contrast to MTRNR2L8, which is long known to be translated into peptides, MTRNR2L12 was initially assumed to be a pseudogene [10]. More recently, MTRNR2L12 was found to be

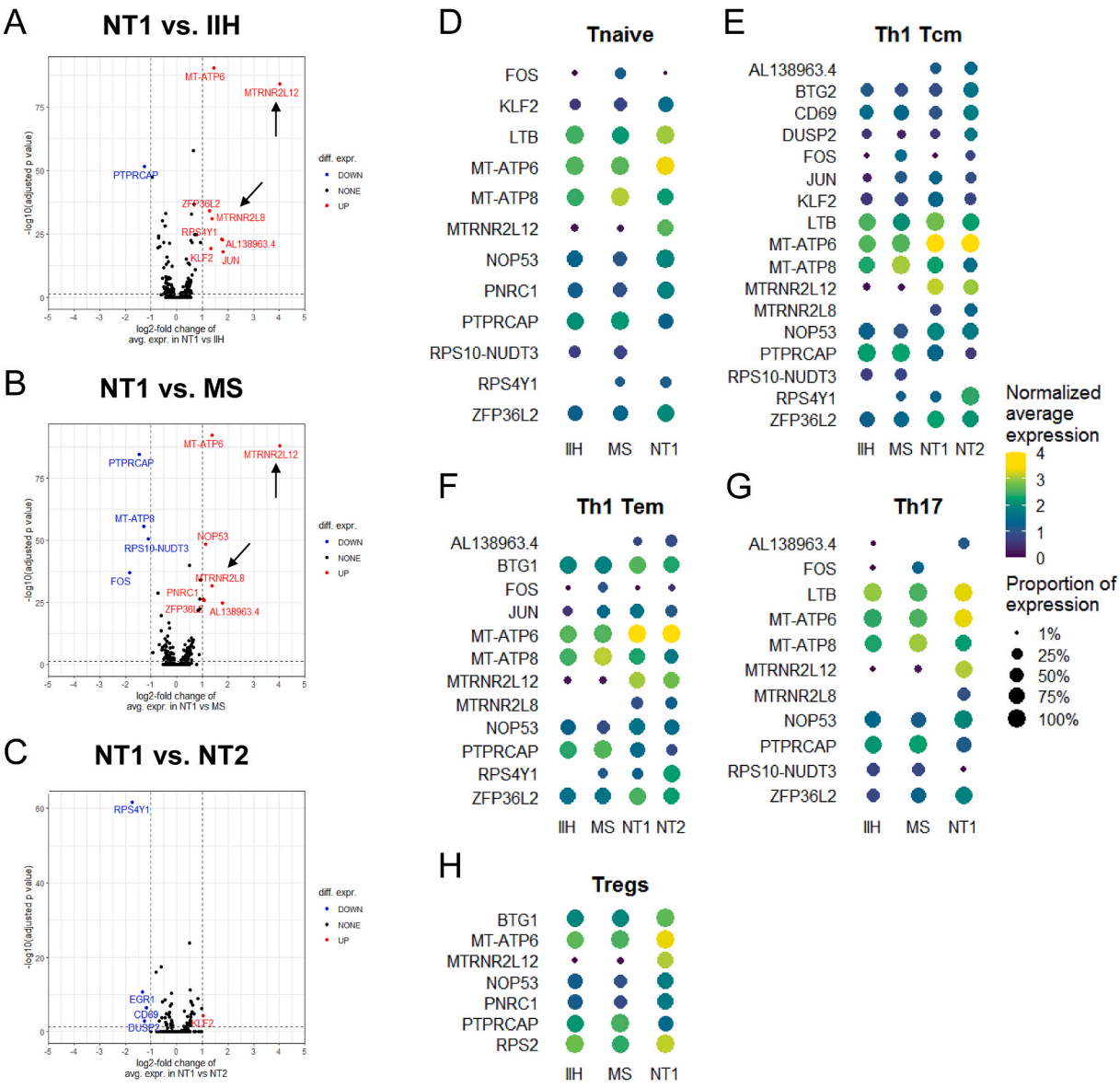

Fig. 6. Analysis of DEG in CD4$^+$ T cells in CSF. Comparison of NT1 versus **A:** IIH, **B:** MS, and **C:** NT2 presented as volcano plots. CD4$^+$ T cells were downsampled to 100 cells per sample to give equal weight to each sample. Samples that contained less than 100 cells remained unchanged. Genes that were upregulated in NT1 as compared to IIH, MS, and NT2 are printed in red, while downregulated genes are shown in blue font. MTRNR2L12 and MTRNR2L8 are indicated by black arrows. **D - H:** Dot plots of DEG of different CD4$^+$ subtypes. **D:** naïve T cells (Tnaive), **E:** Th1 central memory (Th1 Tcm), **F:** Th1 effector memory (Th1 Tem), **G:** Th17 (Th17), and **H:** regulatory (Th1 Treg) T cells. The sizes of the dots are comparable for all cell types and represent the percentage of cells in the cell type expressing each gene. The color of each dot indicates the average expression level in cells of the cell type.

expressed at the RNA level in several tissues including the brain [26]. The high expression of MTRNR2L12 and MTRNR2L8 in narcoleptic patients is particularly intriguing because significant gene expression was detected neither in CSF cells of the inflammatory disease MS nor in the non-inflammatory disease IIH.

HUMANIN is intensely investigated because of its neuroprotective and anti-apoptotic effects in Alzheimer's disease [11]. Although the exchange of leucine to serine is slightly non-conservative, peptides from the HUMANIN gene family were assumed to share anti-apoptotic function [10]. One may speculate that this known link of HUMANIN to Alzheimer's disease and of MTRNR2L12/MTRNR2L8 to NT1, as observed here, might be related to the reported negative association between these two diseases [27]. β-Amyloid dynamics are regulated by hypocretin and the sleep-wake cycle [28], and some studies have highlighted correlations between hypocretin and β-amyloid levels in patients with Alzheimer's disease [29]. Also, lower brain amyloid burden assessed by positron emission tomography was identified in elderly patients with NT1, suggesting a lower risk of amyloidopathy related to Alzheimer's disease [30]. Further, a pathophysiological role of HUMANIN was detected in other diseases, including several neurodegenerative disorders [31–33]. MTRNR2L12 was found to be involved in Hirschsprung's disease, which is a genetic disorder of neural crest development [34]. Taken together, these observations suggest an important role of peptides from the HUMANIN gene-family in the pathophysiology of narcolepsy.

A drawback of our study is that HUMANIN was not enclosed in the reference genome GRCh38-2020-A. Thus, in addition or instead of MTRNR2L12 and -L8, HUMANIN may be a highly relevant DEG. Thus, it will have to be determined whether MTRNR2L12 and -L8, or HUMANIN or all three gene-products are players in the pathogenesis of narcolepsy. Another shortcoming is the low CSF cell numbers that were available for analyses. This is particularly true for NT1 and NT2 because the cell

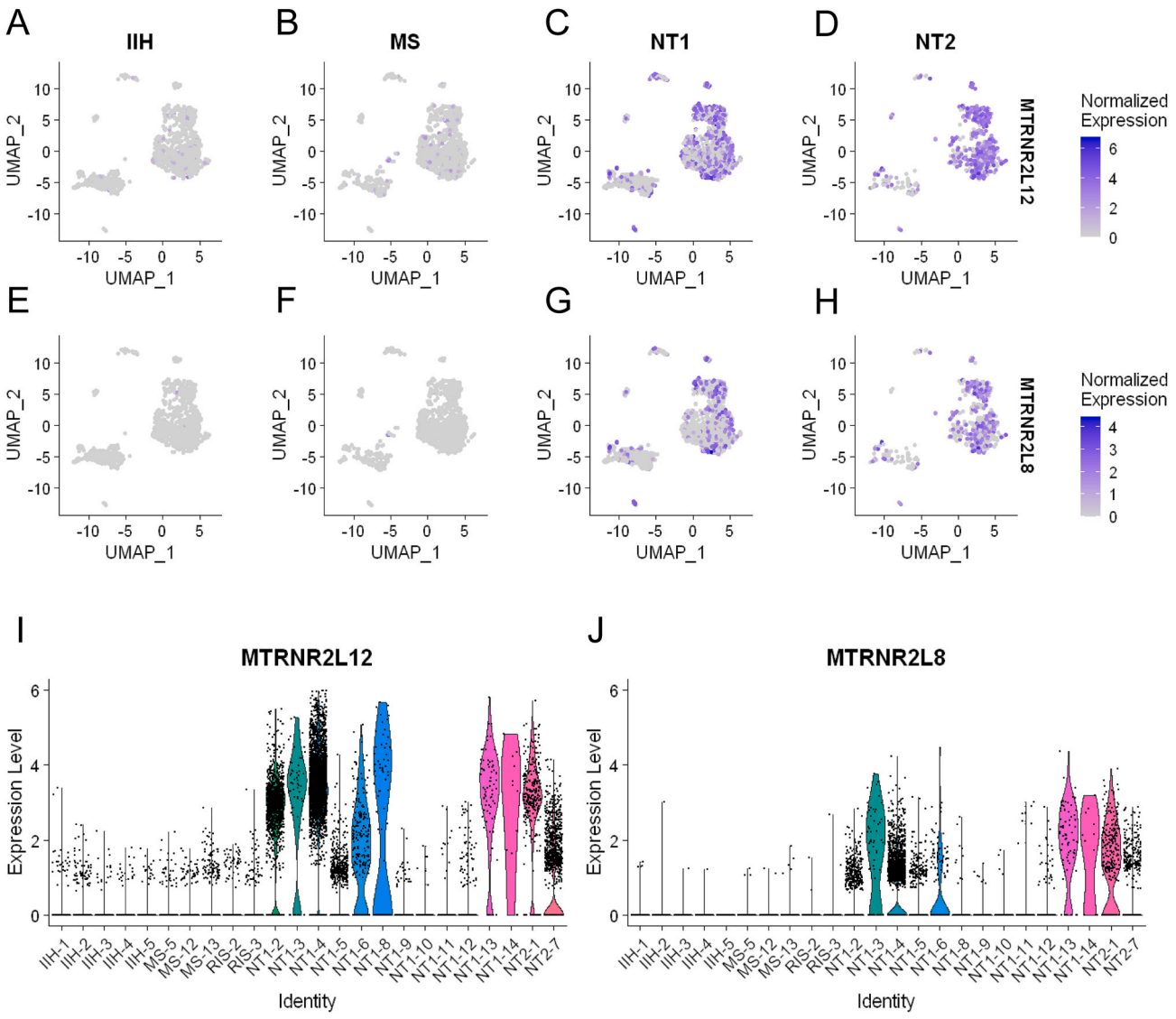

Fig. 7. Expression of MTRNR2L12 and MTRNR2L8. A–H: UMAPs showing expression of MTRNR2L12 in **A:** IIH, **B:** MS, **C:** NT1, and **D:** NT2 patients, and expression of MTRNR2L8 in **E:** IIH, **F:** MS, **G:** NT1, and **H:** NT2 patients. Each sample was down-sampled to 300 cells. In order to give similar weight to the samples with vastly different cell numbers. Dark blue dots indicate cells that express the respective gene, light grey dots indicate cells that do not express the respective gene. **I, J:** Violin plots of each patient of each disease group show that **I:** MTRNR2L12 is strongly expressed in 7 out of 12 NT1-and in 2 out of 2 NT2-patients (NT1-2, −3, −4, −6, −8, −13, −14, and NT2-1, −2), and **J:** MTRNR2L8 is strongly expressed in 5 out of 12 NT1-and in 1 out of 2 NT2-patients (NT1-3, −4, −6, −13, −14, and NT2-1).

numbers per volume is similar to that of healthy individuals, while they are elevated in MS. In IIH, the cell numbers per volume are also low, but higher CSF volumes were obtained for therapeutic reasons. We included 12 hypocretin-deficient patients with NT1 all but one carrying *HLA-DQB1*06:02*, and two patients with NT2 including one with atypical cataplexy and intermediate hypocretin levels as well as *HLA-DQB1*06:02*-positivity, thus with some typical narcolepsy features as recently reported [35]. Only one patient with IIH is *HLA-DQB1*06:02* positive. Nevertheless, we could detect gene expression signatures that were specific for narcolepsy, indicating that the milieu in CSF is less inflammatory than in MS and resembles more the milieu in IIH. Of important note, all narcoleptic patients were recruited very close to disease onset. Further, our unexpected finding that HUMANIN family members were specifically expressed in CSF cells of NT1 and NT2 patients might open the path for functional studies to further elucidate their role in the pathogenesis of narcolepsy. Such functional studies, however, will be hampered by the fact that no close homologues to HUMANIN and the MTRNR2-family are encoded in the genomes of mice.

Author contributions

AH designed and performed research, analyzed data, and contributed to writing the manuscript. IA performed research, analyzed data and contributed to writing. LB performed research, analyzed data and contributed new reagents. LAG performed research, analyzed data and contributed new reagents. DS performed research. SK performed research. HB performed research. HT contributed new reagents. JH contributed new reagents. BW contributed new reagents. TK contributed new reagents. EB performed research and analyzed data. RSL designed research, analyzed data, and contributed to writing the manuscript. YD designed research, analyzed data, contributed new reagents and to writing the manuscript. KD designed research, analyzed data, and wrote the manuscript.

Data availability

Data will be made available on request.

Acknowledgments

We thank all study participants: patients, their families, and the French Association of Narcoleptic patients (*ANC, Association Française de Narcolepsie Cataplexie et d'Hypersomnies rares*). We also thank all the collaborators in the National Reference Center for Narcolepsy, Montpellier, France, especially Jerome Tanty for the biological sampling of narcoleptic patients and Laurent Journot (MGX, Montpellier) for valuable discussion.

This study was supported by the European Community grant ERARE18-052 NARCOMICS, the Foundation pour la Recherche Médicale (grant EQU202203014690), the German Federal Ministry of Education and Research grant 01GM1915, and the German Research Foundation grants DO 420/7-1 and EXC 2145 (SyNergy) – ID 390857198 (LAG, KD and EB). MGX acknowledges financial support from France Génomique National infrastructure, funded as part of "Investissement d'Avenir" program managed by Agence Nationale pour la Recherche (contract ANR-10-INBS-09).

Appendix A. Supplementary data

Supplementary data to this article can be found online at https://doi.org/10.1016/j.jaut.2024.103234.

References

[1] L. Pérez-Carbonell, E. Mignot, G. Leschziner, Y. Dauvilliers, Understanding and approaching excessive daytime sleepiness, Lancet 400 (2022) 1033–1046, https://doi.org/10.1016/S0140-6736(22)01018-2.

[2] C.L.A. Bassetti, A. Adamantidis, D. Burdakov, F. Han, S. Gay, U. Kallweit, R. Khatami, F. Koning, B.R. Kornum, G.J. Lammers, R.S. Liblau, P.H. Luppi, G. Mayer, T. Pollmächer, T. Sakurai, F. Sallusto, T.E. Scammell, M. Tafti, Y. Dauvilliers, Narcolepsy — clinical spectrum, aetiopathophysiology, diagnosis and treatment, Nat. Rev. Neurol. 15 (2019) 519–539, https://doi.org/10.1038/s41582-019-0226-9.

[3] R.S. Liblau, D. Latorre, B.R. Kornum, Y. Dauvilliers, E.J. Mignot, The immunopathogenesis of narcolepsy type 1, Nat. Rev. Immunol. (2024) 33–48, https://doi.org/10.1038/s41577-023-00902-9.

[4] L. Barateau, F. Pizza, G. Plazzi, Y. Dauvilliers, Narcolepsy, J. Sleep Res. 31 (2022), https://doi.org/10.1111/jsr.13631.

[5] T.O. Sarkanen, A.P.E. Alakuijala, Y.A. Dauvilliers, M.M. Partinen, Incidence of narcolepsy after H1N1 influenza and vaccinations: systematic review and meta-analysis, Sleep Med. Rev. 38 (2018) 177–186, https://doi.org/10.1016/j.smrv.2017.06.006.

[6] H.M. Ollila, E. Sharon, L. Lin, N. Sinnott-Armstrong, A. Ambati, S.M. Yogeshwar, R. P. Hillary, O. Jolanki, J. Faraco, M. Einen, G. Luo, J. Zhang, F. Han, H. Yan, X. S. Dong, J. Li, J. Zhang, S.-C. Hong, T.W. Kim, Y. Dauvilliers, L. Barateau, G. J. Lammers, R. Fronczek, G. Mayer, J. Santamaria, I. Arnulf, S. Knudsen-Heier, M. K.L. Bredahl, P.M. Thorsby, G. Plazzi, F. Pizza, M. Moresco, C. Crowe, S.K. Van Den Eeden, M. Lecendreux, P. Bourgin, T. Kanbayashi, F.J. Martínez-Orozco, R. Peraita-Adrados, A. Benetó, J. Montplaisir, A. Desautels, Y.-S. HuangFinnGen, T.D. Als, A. Ziemann, A. Abbasi, A. Lehtonen, A. Lertratanakul, B. Riley-Gillis, F. Rahimov, H. Jacob, J. Waring, M. Liu, N. Smaoui, R. Popovic, A. Platt, A. Matakidou, B. Challis, D. Paul, G. Lassi, I. Tachmazidou, A. Hakanen, J. Schleutker, N. Pitkänen, P. Terho, P. Virolainen, A. Mannermaa, V.-M. Kosma, C.-Y. Chen, H. Runz, S. John, S. Lahdenperä, S. Loomis, S. Eaton, G. Okafo, H. Salminen-Mankonen, M. Jung, N. Lawless, Z. Ding, J. Maranville, M. Hochfeld, R. Plenge, S. Biswas, M. Kanai, M. Maasha, W. Zhou, O. Tuovila, R. Pakkanen, J. Laukkanen, T. Kuopio, K. Aittomäki, A. Mäkitie, N. Pujol, T. Laisk, K. Aalto-Setälä, J. Mäkelä, M. Hautalahti, S. Smith, T. Southerington, E. Kangasniemi, H. Palin, M. Kähönen, S. Siltanen, T. Laitinen, F. Vaura, J. Suvisaari, T. Niiranen, V. Salomaa, J. Partanen, M. Arvas, J. Ritari, K. Hyvärinen, D. Choy, E. Teng, E. Strauss, H. Chen, H. Chen, J. Schutzman, J. Hunkapiller, M. McCarthy, N. Bowers, R. Pendergrass, T. Lu, A. Chu, D. Kulkarni, F. Xu, J. Betts, J. Eicher, J.E. Gordillo, L. Addis, L. McCarthy, R. Mishra, J. Kumar, M.G. Ehm, K. Auro, D. Pulford, A. Pitkäranta, A. Loukola, E. Punkka, M.-M. Linna, O. Carpén, T. Raivio, J.A. Turunen, T.P. Mäkelä, A. Salminen, A. Aarnisalo, D. Gordin, D. Rice, E. Isometsä, E. Salminen, H. Joensuu, I. Kalliala, J. Mattson, J. Sinisalo, J. Koskela, K. Eklund, K. Hannula-Jouppi, L. Aaltonen, M.-R. Taskinen, M. Färkkilä, M. Raivio, O. Heikinheimo, P. Kauppi, P. Nieminen, P. Tienari, P. Pussinen, S. Pikkarainen, T. Ollila, T. Tuomi, T. Hiltunen, T. Meretoja, T. Salo, U. Palotie, A. Palomäki, J. Aittokallio, J. Rinne, K. Metsärinne, K. Elenius, L. Pirilä, L. Koulu, M. Voutilainen, R. Lahesmaa, R. Kallionpää, S. Peltonen, T. Willberg, U. Gursoy, V. Jokimaa, A. Palotie, A. Kytölä, A. Ganna, A. Jalanko, A. Liu, A. Lehisto, A. Ghazal, E. Kilpeläinen, E. Widen, E. Saarentaus, E. Pitkänen, H. Ollila, H. Laivuori, H. Heyne, H.-Y. Shen, J. Kaprio, J. Rämö, J. Karjalainen, J. Mehtonen, J. Pitkänen, K. Pärn, K. Donner, K. Kivinen, L.E. Lahtela, M.E. Niemi, M. Kaunisto, M. Kals, M.P. Reeve, M. Aavikko, N. Mars, O.A. Dada, P. Della Briotta Parolo, P. Palta, R. Weldatsadik, R. Kajanne, R. Rodosthenous, S. Ripatti, S. Ruotsalainen, S. Strausz, S. Hassan, S. S. Padmanabhuni, S. Luo, S. Lemmelä, T. Tukiainen, T.P. Sipilä, T. Kiiskinen, V. Llorens, M. Daly, J. Lee, K. Tsuo, M. Kurki, A. Elliott, A. Havulinna, J. Partanen, R. Yang, D. Reilly, A. Porello, A. Hart, D. Waterworth, E. Khramtsova, K. He, M. Guan, Q.S. Li, S. Vuoti, E. Green, R. Graham, S. Mozaffari, A. Huertas-Vazquez, A. Loboda, C. Fox, F. Farias, J.-H. Sul, J. Miller, N. Raghavan, S. Longerich, J. Kettunen, R. Serpi, R. Hinttala, T. Mantere, A. Remes, E. Rahikkala, J. Huhtakangas, K. Tasanen, L. Huilaja, L. Morin-Papunen, M. Niinimäki, M. Vääräsmäki, O. Uimari, P. Karihtala, T. Piltonen, T. Harju, T. Blomster, V. Anttonen, H. Soininen, K. Kaarniranta, L. Suominen, M. Pelkonen, M. Siponen, M. Kiviniemi, O. Kaipiainen-Seppänen, P. Auvinen, P. Mäntylä, R. Kälviäinen, V. Julkunen, C. O'Donnell, M. Obeidat, N. Renaud, D. Ngo, M. Mouded, M. Mendelson, A. Mälarstig, H. Lehtonen, J. Parkkinen, K. Kalpala, M. Miller, N. Bing, S. McDonough, X. Hu, Y. Wu, A. Jussila, A. Auranen, A. Bizaki-Vallaskangas, H. Uusitalo, J. Peltola, J. Hernesniemi, K. Kaukinen, L. Kotaniemi-Talonen, P. Isomäki, T. Salmi, V. Kurra, K. Sipilä, A. Toivola, E. Järvensivu, E. Kaiharju, H. Mattsson, K. Kristiansson, L. Männikkö, M. Laukkanen, M. Perola, M. Brunfeldt, P. Laiho, R. Wong, S. Koskelainen, S. Lähteenmäki, S. Soini, T. Paajanen, T. Kilpi, T. Hiekkalinna, T. Sistonen, C. Chatelain, D. Raipal, K. Klinger, S. Lessard, F. Åberg, M. Hiltunen, S. Heikkinen, H. Kankaanranta, T. Palotie, I. Hovatta, K. Palin, N. Välimäki, S. Toppila-Salmi, E. Laakkonen, E. Sliz, H. Silven, K. Pylkäs, M. Karjalainen, R. Arffman, S. Savukoski, J. Tyrmi, M. Rivas, H. Siirtola, I. Vähätalo, J. Garcia-Tabuenca, M. Niemi, M. Helminen, T. Luukkaala, P. Jennum, S. Nevsimalova, D. Kemlink, A. Iranzo, S. Overeem, A. Wierzbicka, P. Geisler, K. Sonka, M. Honda, B. Högl, A. Stefani, F.M. Coelho, V. Mantovani, E. Feketeova, M. Wadelius, N. Eriksson, H. Smedje, P. Hallberg, P.E. Hesla, D. Rye, Z. Pelin, L. Ferini-Strambi, C.L. Bassetti, J. Mathis, R. Khatami, A. Aran, S. Nampoothiri, T. Olsson, I. Kockum, M. Partinen, M. Perola, B.R. Kornum, S. Rueger, J. Winkelmann, T. Miyagawa, H. Toyoda, S.-S. Khor, M. Shimada, K. Tokunaga, M. Rivas, J.K. Pritchard, N. Risch, Z. Kutalik, R. O'Hara, J. Hallmayer, C.J. Ye, E.J. Mignot, Narcolepsy risk loci outline role of T cell autoimmunity and infectious triggers in narcolepsy, Nat. Commun. 14 (2023) 2709, https://doi.org/10.1038/s41467-023-36120-z.

[7] E. Beltrán, X.-H. Nguyen, C. Quériault, L. Barateau, Y. Dauvilliers, K. Dornmair, R. S. Liblau, Shared T cell receptor chains in blood memory CD4+ T cells of narcolepsy type 1 patients, J. Autoimmun. 100 (2019) 1–6, https://doi.org/10.1016/j.jaut.2019.03.010.

[8] D. Latorre, U. Kallweit, E. Armentani, M. Foglierini, F. Mele, A. Cassotta, S. Jovic, D. Jarrossay, J. Mathis, F. Zellini, B. Becher, A. Lanzavecchia, R. Khatami, M. Manconi, M. Tafti, C.L. Bassetti, F. Sallusto, T cells in patients with narcolepsy target self-antigens of hypocretin neurons, Nature 562 (2018) 63–68, https://doi.org/10.1038/s41586-018-0540-1.

[9] G. Luo, J. Zhang, L. Lin, E.J.-M. Mignot, Characterization of T cell receptors reactive to HCRT $_{NH2}$, pHA $_{273-287}$, and NP $_{17-31}$ in control and narcolepsy patients, Proc. Natl. Acad. Sci. U.S.A. 119 (2022) e2205797119, https://doi.org/10.1073/pnas.2205797119.

[10] M. Bodzioch, K. Lapicka-Bodzioch, B. Zapala, W. Kamysz, B. Kiec-Wilk, A. Dembinska-Kiec, Evidence for potential functionality of nuclearly-encoded humanin isoforms, Genomics 94 (2009) 247–256, https://doi.org/10.1016/j.ygeno.2009.05.006.

[11] Y. Hashimoto, T. Niikura, H. Tajima, T. Yasukawa, H. Sudo, Y. Ito, Y. Kita, M. Kawasumi, K. Kouyama, M. Doyu, G. Sobue, T. Koide, S. Tsuji, J. Lang, K. Kurokawa, I. Nishimoto, A rescue factor abolishing neuronal cell death by a wide spectrum of familial Alzheimer's disease genes and Aβ, Proc. Natl. Acad. Sci. U.S.A. 98 (2001) 6336–6341, https://doi.org/10.1073/pnas.101133498.

[12] A. Agrafiotis, R. Dizerens, I. Vincenti, I. Wagner, R. Kuhn, D. Shlesinger, M. Manero-Carranza, T.-S. Cotet, K.-L. Hong, N. Page, N. Fonta, G. Shammas, A. Mariotte, M. Piccinno, M. Kreutzfeldt, B. Gruntz, R. Ehling, A. Genovese, A. Pedrioli, A. Dounas, S. Franzenburg, H. Tumani, T. Kümpfel, V. Kavaka, L. A. Gerdes, K. Dornmair, E. Beltrán, A. Oxenius, S.T. Reddy, D. Merkler, A. Yermanos, Persistent virus-specific and clonally expanded antibody-secreting cells respond to induced self-antigen in the CNS, Acta Neuropathol. 145 (2023) 335–355, https://doi.org/10.1007/s00401-023-02537-5.

[13] A. Kendirli, C. De La Rosa, K.F. Lämmle, K. Eglseer, I.J. Bauer, V. Kavaka, S. Winklmeier, L. Zhuo, C. Wichmann, L.A. Gerdes, T. Kümpfel, K. Dornmair, E. Beltrán, M. Kerschensteiner, N. Kawakami, A genome-wide in vivo CRISPR screen identifies essential regulators of T cell migration to the CNS in a multiple sclerosis model, Nat. Neurosci. 26 (2023) 1713–1725, https://doi.org/10.1038/s41593-023-01432-2.

[14] H. Touil, T. Roostaei, D. Calini, C. Diaconu, S. Epstein, C. Raposo, K. Onomichi, K. T. Thakur, L. Craveiro, I. Callegari, J. Bryois, C.S. Riley, V. Menon, T. Derfuss, P. L. De Jager, D. Malhotra, A structured evaluation of cryopreservation in generating single-cell transcriptomes from cerebrospinal fluid, Cell Reports Methods 3 (2023) 100533, https://doi.org/10.1016/j.crmeth.2023.100533.

[15] K. Deschler, J. Rademacher, S.M. Lacher, A. Huth, M. Utzt, S. Krebs, H. Blum, H. Haibel, F. Proft, M. Protopopov, V.R. Rodriguez, E. Beltrán, D. Poddubnyy, K. Dornmair, Antigen-specific immune reactions by expanded CD8+ T cell clones from HLA-B*27-positive patients with spondyloarthritis, J. Autoimmun. 133 (2022) 102901, https://doi.org/10.1016/j.jaut.2022.102901.

[16] G.X.Y. Zheng, J.M. Terry, P. Belgrader, P. Ryvkin, Z.W. Bent, R. Wilson, S. B. Ziraldo, T.D. Wheeler, G.P. McDermott, J. Zhu, M.T. Gregory, J. Shuga, L. Montesclaros, J.G. Underwood, D.A. Masquelier, S.Y. Nishimura, M. Schnall-Levin, P.W. Wyatt, C.M. Hindson, R. Bharadwaj, A. Wong, K.D. Ness, L.W. Beppu, H.J. Deeg, C. McFarland, K.R. Loeb, W.J. Valente, N.G. Ericson, E.A. Stevens, J. P. Radich, T.S. Mikkelsen, B.J. Hindson, J.H. Bielas, Massively parallel digital

transcriptional profiling of single cells, Nat. Commun. 8 (2017) 14049, https://doi.org/10.1038/ncomms14049.
[17] M. Hiltensperger, E. Beltrán, R. Kant, S. Tyystjärvi, G. Lepennetier, H. Domínguez Moreno, I.J. Bauer, S. Grassmann, S. Jarosch, K. Schober, V.R. Buchholz, S. Kenet, C. Gasperi, R. Öllinger, R. Rad, A. Muschaweckh, C. Sie, L. Aly, B. Knier, G. Garg, A. M. Afzali, L.A. Gerdes, T. Kümpfel, S. Franzenburg, N. Kawakami, B. Hemmer, D. H. Busch, T. Misgeld, K. Dornmair, T. Korn, Skin and gut imprinted helper T cell subsets exhibit distinct functional phenotypes in central nervous system autoimmunity, Nat. Immunol. 22 (2021) 880–892, https://doi.org/10.1038/s41590-021-00948-8.
[18] I. Korsunsky, N. Millard, J. Fan, K. Slowikowski, F. Zhang, K. Wei, Y. Baglaenko, M. Brenner, P. Loh, S. Raychaudhuri, Fast, sensitive and accurate integration of single-cell data with Harmony, Nat. Methods 16 (2019) 1289–1296, https://doi.org/10.1038/s41592-019-0619-0.
[19] R. Reantragoon, A.J. Corbett, I.G. Sakala, N.A. Gherardin, J.B. Furness, Z. Chen, S. B.G. Eckle, A.P. Uldrich, R.W. Birkinshaw, O. Patel, L. Kostenko, B. Meehan, K. Kedzierska, L. Liu, D.P. Fairlie, T.H. Hansen, D.I. Godfrey, J. Rossjohn, J. McCluskey, L. Kjer-Nielsen, Antigen-loaded MR1 tetramers define T cell receptor heterogeneity in mucosal-associated invariant T cells, J. Exp. Med. 210 (2013) 2305–2320, https://doi.org/10.1084/jem.20130958.
[20] T. Wu, E. Hu, S. Xu, M. Chen, P. Guo, Z. Dai, T. Feng, L. Zhou, W. Tang, L. Zhan, X. Fu, S. Liu, X. Bo, G. Yu, clusterProfiler 4.0: a universal enrichment tool for interpreting omics data, Innovation 2 (2021) 100141, https://doi.org/10.1016/j.xinn.2021.100141.
[21] M. Lecendreux, G. Churlaud, F. Pitoiset, A. Regnault, T.A. Tran, R. Liblau, D. Klatzmann, M. Rosenzwajg, Narcolepsy type 1 is associated with a systemic increase and activation of regulatory T cells and with a systemic activation of global T cells, PLoS One 12 (2017) e0169836, https://doi.org/10.1371/journal.pone.0169836.
[22] F.J. Hartmann, R. Bernard-Valnet, C. Quériault, D. Mrdjen, L.M. Weber, E. Galli, C. Krieg, M.D. Robinson, X.-H. Nguyen, Y. Dauvilliers, R.S. Liblau, B. Becher, High-dimensional single-cell analysis reveals the immune signature of narcolepsy, J. Exp. Med. 213 (2016) 2621–2633, https://doi.org/10.1084/jem.20160897.
[23] A. Lind, F. Salami, A. Landtblom, L. Palm, Å. Lernmark, J. Adolfsson, H. Elding Larsson, Immunocyte single cell analysis of vaccine-induced narcolepsy, Eur. J. Immunol. 51 (2021) 247–249, https://doi.org/10.1002/eji.202048633.
[24] I. Ayoub, Y. Dauvilliers, L. Barateau, T. Vermeulen, E. Mouton-Barbosa, M. Marcellin, A. Gonzalez-de-Peredo, C.C. Gross, A. Saoudi, R. Liblau, Cerebrospinal fluid proteomics in recent-onset Narcolepsy type 1 reveals activation of the complement system, Front. Immunol. 14 (2023) 1108682, https://doi.org/10.3389/fimmu.2023.1108682.
[25] B.R. Kornum, F. Pizza, S. Knudsen, G. Plazzi, P. Jennum, E. Mignot, Cerebrospinal fluid cytokine levels in type 1 narcolepsy patients very close to onset, Brain Behav. Immun. 49 (2015) 54–58, https://doi.org/10.1016/j.bbi.2015.03.004.
[26] G.R. Assis-Mendonça, M.C.P. Athié, J.V.G. Tamanini, A. de Souza, G.G. Zanetti, P. A.O.R.A. Araújo, E. Ghizoni, H. Tedeschi, M.K.M. Alvim, V.S.D. Almeida, W. de Souza, R. Coras, C.L. Yasuda, I. Blümcke, A.S. Vieira, F. Cendes, I. Lopes-Cendes, F. Rogerio, Transcriptome analyses of the cortex and white matter of focal cortical dysplasia type II: insights into pathophysiology and tissue characterization, Front. Neurol. 14 (2023) 1023950, https://doi.org/10.3389/fneur.2023.1023950.
[27] Y. Dauvilliers, Hypocretin/orexin, sleep and Alzheimer's disease, in: M.A. Steiner, M. Yanagisawa, M. Clozel (Eds.), Frontiers of Neurology and Neuroscience, S. Karger AG, 2021, pp. 139–149, https://doi.org/10.1159/000514967.
[28] J.-E. Kang, M.M. Lim, R.J. Bateman, J.J. Lee, L.P. Smyth, J.R. Cirrito, N. Fujiki, S. Nishino, D.M. Holtzman, Amyloid-β dynamics are regulated by orexin and the sleep-wake cycle, Science 326 (2009) 1005–1007, https://doi.org/10.1126/science.1180962.
[29] Y.A. Dauvilliers, S. Lehmann, I. Jaussent, A. Gabelle, Hypocretin and brain Î²-amyloid peptide interactions in cognitive disorders and narcolepsy, Front. Aging Neurosci. 6 (2014), https://doi.org/10.3389/fnagi.2014.00119.
[30] A. Gabelle, I. Jaussent, F.B. Bouallègue, S. Lehmann, R. Lopez, L. Barateau, C. Grasselli, C. Pesenti, D. De Verbizier, S. Béziat, D. Mariano-Goulart, B. Carlander, Y. Dauvilliers, The Alzheimer's disease neuroimaging initiative, multi-domain intervention Alzheimer's prevention trial study groups, reduced brain amyloid burden in elderly patients with narcolepsy type 1: amyloid load in narcolepsy, Ann. Neurol. 85 (2019) 74–83, https://doi.org/10.1002/ana.25373.
[31] A. Hazafa, A. Batool, S. Ahmad, M. Amjad, S.N. Chaudhry, J. Asad, H.F. Ghuman, H.M. Khan, M. Naeem, U. Ghani, Humanin: a mitochondrial-derived peptide in the treatment of apoptosis-related diseases, Life Sci. 264 (2021) 118679, https://doi.org/10.1016/j.lfs.2020.118679.
[32] T. Niikura, Humanin and Alzheimer's disease: the beginning of a new field, Biochim. Biophys. Acta Gen. Subj. 1866 (2022) 130024, https://doi.org/10.1016/j.bbagen.2021.130024.
[33] K. Thiankhaw, K. Chattipakorn, S.C. Chattipakorn, N. Chattipakorn, Roles of humanin and derivatives on the pathology of neurodegenerative diseases and cognition, Biochim. Biophys. Acta Gen. Subj. 1866 (2022) 130097, https://doi.org/10.1016/j.bbagen.2022.130097.
[34] C. Du, H. Xie, R. Zang, Z. Shen, H. Li, P. Chen, X. Xu, Y. Xia, W. Tang, Apoptotic neuron-secreted HN12 inhibits cell apoptosis in Hirschsprung's disease, IJN 11 (2016) 5871–5881, https://doi.org/10.2147/IJN.S114838.
[35] E. Postiglione, L. Barateau, F. Pizza, R. Lopez, E. Antelmi, A.-L. Rassu, S. Vandi, S. Chenini, E. Mignot, Y. Dauvilliers, G. Plazzi, Narcolepsy with intermediate cerebrospinal level of hypocretin-1, Sleep 45 (2022), https://doi.org/10.1093/sleep/zsab285 zsab285.